

The critical surface of the $SU(3)_L \times SU(3)_R$ chiral quark model at non-zero baryon density

P. Kovács*

Department of Atomic Physics, Eötvös University, H-1117 Budapest, Hungary

Zs. Szép†

Research Institute for Solid State Physics and Optics of the Hungarian Academy of Sciences, H-1525 Budapest, Hungary

The boundary of the first order chiral phase transition region is studied in the $m_\pi - m_K - \mu_B$ space using the one-loop optimized perturbation theory for the resummation of the perturbative series. Chiral perturbation theory for mesons and baryons is used for the $T = 0$ parametrization of the model. The surface of second order transition points bends with increasing μ_B towards the physical point of the $m_\pi - m_K$ mass plane allowing for the existence of the critical end point in the $\mu_B - T$ plane at the physical point. The location and scaling region of the CEP is explored.

PACS numbers: 11.10.Wx, 11.30.Rd, 12.39.Fe

I. INTRODUCTION

In the past few years much effort was invested in the mapping of the phase diagram of strongly interacting matter. Apart from the theoretical importance of the phase transition for understanding of the physics of the early universe the continuous interest in this issue is also triggered by the fact that some parts of the phase diagram are within the reach of current and future heavy ion collision experiments. In QCD and also in its effective models the parameter space contains both experimentally tunable quantities like the temperature and various chemical potentials (isospin, strange, baryonic) and parameters like the quark masses which have a fixed value in nature (physical point). At zero chemical potential the nature of the phase transition at the physical point was established only very recently. The continuum extrapolation in the lattice investigation of Refs. [1, 2] using staggered fermions showed that the transition is of analytic cross-over type. How far the physical point is located from the boundary of the first order transition region, expected on theoretical grounds in the limit of vanishing quark masses, is not yet definitively quantified. Both lattice simulations with improved staggered quarks (p4 action) [3] and effective model studies [4, 5, 6, 7] show that for degenerate quark masses the first order transition region extends to pseudo-Goldstone meson masses with values well below the physical mass of the pion.

For non-vanishing baryonic chemical potential the first order transition region persists and its second order boundary forms a critical surface in the $m_{u,d} - m_s - \mu_B$ space on which the transition as a function of temperature is of second order. Generally it is expected that for high values of the chemical potential the phase transition is of first order, so that the critical surface bends towards the physical point (positive curvature). In this case at physical quark masses there is a critical end point (CEP) in the chemical potential-temperature plane at which the first order transition line ends. In this plane, for chemical potential values smaller than the value at CEP the phase transition changes to a cross-over. The CEP was found in staggered lattice QCD first for a non-physical value of m_{ud} [8] and then for physical values of the quark masses [9] (pion to rho meson masses tuned to its physical value). The location of the CEP was also estimated in Ref. [10] using Taylor expansion around $\mu_B = 0$. However, the question of the existence and location of the CEP is not yet settled for two reasons. First the continuum extrapolation is not yet performed and not all the lattice methods used to address the notoriously difficult problem of performing simulations at finite chemical potential could find the CEP. According to the simulation of Ref. [11] performed with imaginary chemical potential the critical surface turns out to be extremely quark mass sensitive and contrary to the standard expectation seems to have negative curvature (the first order transition region shrinks with increasing μ_B). This would imply the absence of the CEP in the validity range of the method used in Ref. [11] estimated to be $\mu_B < 500$ MeV, but leave the possibility of its appearance above this limiting value.

In this paper our aim is to study the phase boundary of the first order transition region of the chiral phase transition in the $m_\pi - m_K - \mu_B$ space with special interest for the location of the critical end point in the $\mu_B - T$ -plane occurring at the physical point of the mass-plane. For this investigation the $SU(3)_L \times SU(3)_R$ chiral quark model [12] is used as an effective model of strong interactions. This model has the same global symmetry features as the QCD. In view of the result of [11] which shades doubts on the existence of the CEP, we investigate thoroughly, by studying the predicted mass spectrum, how reliable is the existence of the CEP predicted by our model (Sec. II). Then by continuing the

*Electronic address: kpeti@cleopatra.elte.hu

†Electronic address: szepzs@achilles.elte.hu

parameters of the model as functions of m_π and m_K using the chiral perturbation theory (CHPT) for meson and baryons we study the shape of the critical surface which bounds the region of chiral first order transitions in the $m_\pi - m_K - \mu_B$ space (Sec. III A). For physical values of m_π and m_K the location of the CEP in the $\mu_B - T$ plane will be determined in Sec. III B. We conclude in Sec. IV.

II. THE MODEL AND THE DETERMINATION OF ITS PARAMETERS

The Lagrangian of the $SU(3)_L \times SU(3)_R$ symmetric chiral quark model containing explicit symmetry breaking terms is given by

$$L = \frac{1}{2} \text{Tr} (\partial_\mu M^\dagger \partial^\mu M + m_0^2 M^\dagger M) - f_1 (\text{Tr} (M^\dagger M))^2 - f_2 \text{Tr} (M^\dagger M)^2 - g (\det(M) + \det(M^\dagger)) + \epsilon_0 \sigma_0 + \epsilon_8 \sigma_8 + \bar{\psi} (i \not{\partial} - g_F M_5) \psi. \quad (1)$$

The quark field $\bar{\psi} = (u, d, s)$ has implicit Dirac and color indices. The two 3×3 complex matrices are defined in terms of the scalar σ_i and pseudoscalar π_i fields as $M = \frac{1}{\sqrt{2}} \sum_{i=0}^8 (\sigma_i + i\pi_i) \lambda_i$ and $M_5 = \sum_{i=0}^8 \frac{1}{2} (\sigma_i + i\gamma_5 \pi_i) \lambda_i$, with $\lambda_i : i = 1 \dots 8$ the Gell-Mann matrices and $\lambda_0 := \sqrt{\frac{2}{3}} \mathbf{1}$. From the original 0-8 basis we switch to the non-strange (x) - strange (y) basis by performing the orthogonal transformation

$$\begin{pmatrix} v_x \\ v_y \end{pmatrix} = \frac{1}{\sqrt{3}} \begin{pmatrix} \sqrt{2} & 1 \\ 1 & -\sqrt{2} \end{pmatrix} \begin{pmatrix} v_0 \\ v_8 \end{pmatrix}, \quad (2)$$

applied to the scalar, pseudoscalar mesons and external fields, that is $v \in \{\sigma, \pi, \epsilon\}$. Then one has

$$M_5 = \frac{1}{\sqrt{2}} \sum_{i=1}^7 (\sigma_i + i\gamma_5 \pi_i) \lambda_i + \frac{1}{\sqrt{2}} \text{diag}(\sigma_x + i\gamma_5 \pi_x, \sigma_x + i\gamma_5 \pi_x, \sqrt{2}(\sigma_y + i\gamma_5 \pi_y)), \quad (3)$$

and similarly for M .

In the broken phase the fields are shifted with their expectation values $x := \langle \sigma_x \rangle$ and $y := \langle \sigma_y \rangle$, which are obtained from $\langle \sigma_0 \rangle$ and $\langle \sigma_8 \rangle$ cf. Eq. (2). No isospin breaking is considered which means that the u and d constituent quarks are degenerate in mass: $M_u = M_d = g_F x / 2$. The mass of the strange constituent quark is $M_s = g_F y / \sqrt{2}$. The explicit expression for the mesonic sector of the Lagrangian obtained after performing the traces can be found in [13, 14]. The sum of terms linear in the fluctuations gives two equations of state which at one-loop level are

$$0 = \left\langle \frac{\partial L}{\partial \sigma_x} \right\rangle = -\epsilon_x - m_0^2 x + 2gxy + 4f_1 xy^2 + 2(2f_1 + f_2)x^3 + \sum_{\alpha, i, j} t_{\alpha, i, j}^x \langle \alpha_i \alpha_j \rangle + \frac{g_F}{2} (\langle \bar{u}u \rangle + \langle \bar{d}d \rangle), \quad (4)$$

$$0 = \left\langle \frac{\partial L}{\partial \sigma_y} \right\rangle = -\epsilon_y - m_0^2 y + gx^2 + 4f_1 x^2 y + 4(f_1 + f_2)y^3 + \sum_{\alpha, i, j} t_{\alpha, i, j}^y \langle \alpha_i \alpha_j \rangle + \frac{g_F}{\sqrt{2}} \langle \bar{s}s \rangle, \quad (5)$$

where α goes over the pseudoscalar and scalar fields and $i \in \{1 \dots 7, x, y\}$. The non-zero three-point couplings $t_{\alpha, i, j}^x$ and $t_{\alpha, i, j}^y$ are given in Appendix C of Ref. [6]. Note, that in a given multiplet the three-point couplings are degenerate, e.g. $t_{11}^\pi = t_{22}^\pi = t_{33}^\pi$. The coefficients of the quadratic terms in the fluctuations are the tree-level masses (see Table 1 of [7]). The mixing in the $x - y$ (0 - 8) sector is reflected by the fact that the off-diagonal xy component of the mass matrix is non-vanishing. In Appendix A we sketch how the propagators of the mass eigenvalues (η, η' and σ, f_0) are obtained.

In Ref. [7] a method was proposed to determine the parameters of the Lagrangian. At the core of this procedure there is a resummation performed using the so-called Optimized Perturbation Theory (OPT) of Ref. [15] in order to avoid the appearance of negative propagator mass squares in the finite temperature calculations with one-loop accuracy. In the OPT the mass parameter $-m_0^2$ of the Lagrangian, which could be negative if the model exhibits symmetry breaking, is replaced by an effective (temperature-dependent) mass parameter m^2 :

$$L_{mass} = \frac{1}{2} m^2 \text{Tr} M^\dagger M - \frac{1}{2} (m_0^2 + m^2) \text{Tr} M^\dagger M \equiv \frac{1}{2} m^2 \text{Tr} M^\dagger M - \frac{1}{2} \Delta m^2 \text{Tr} M^\dagger M. \quad (6)$$

m^2 is determined using the criterion of fastest apparent convergence (FAC) and the finite counterterm Δm^2 is taken into account first at one-loop level.

Compared to [7], apart from the fact that we have to fix the Yukawa coupling g_F , we have changed the parametrization in two aspects. 1. In place of the one-loop relations of the Partially Conserved Axial-Vector Current (PCAC) we use only the tree-level relation for the pion decay constant, because it turned out that in contrast to the one loop-bosonic contributions, which are explicitly renormalization scale independent, the fermionic contribution depends on the fermionic renormalization scale. 2. We have modified the gap equation for the pions and defined the one-loop

pion mass as $-iG^{-1}(p=0) = M_\pi^2$ instead of defining it as a pole-mass. This is because previous investigations [7, 15] showed that an unavoidable feature of the OPT method is that at finite temperature the solutions of the gap equation and of the equations of state cease to exist above a certain temperature, unless we impose arbitrarily that the finite temperature part of the mesonic bubble integral is taken at vanishing external momentum.

In what follows we present the equations used to determine at $T = 0$ the 9 parameters of the Lagrangian: the couplings m_0^2, f_1, f_2, g, g_F , the condensates x, y and the external fields ϵ_x, ϵ_y . The physical content of the one-loop pseudoscalar self-energies are shown diagrammatically in Fig. 1 of [7], here we give explicitly only the fermionic contributions. The integrals are given in Appendix B. The renormalization of the mesonic part was discussed in [7] where the counterterms $\delta m_0^2, \delta g, \delta f_1$ and δf_2 were given by Eqs. (4)-(7). Since the fermions are taken into account perturbatively one can easily see from Eqs. (4) and (5) that using cut-off regularization the renormalization of the momentum-independent fermionic parts can be achieved with the following counterterms

$$\delta m_0^{2,F} = -\frac{g_f^2}{8\pi^2}\Lambda^2, \quad \delta f_2^F = -\frac{g_F^4}{64\pi^2} \ln \frac{\Lambda^2}{l_f^2}. \quad (7)$$

Λ is the 3d cut-off. The renormalization of the momentum-dependent fermionic parts can be achieved with a wave function renormalization constant in the mesonic sector: $\delta Z = -\frac{g_F^2}{16\pi^2} \ln \frac{\Lambda^2}{l_f^2}$.

The FAC criterion used to determine the effective mass m^2 is implemented by requiring that the one-loop pion mass

$$M_\pi^2 = -m_0^2 + (4f_1 + 2f_2)x^2 + 4f_1y^2 + 2gy + \Sigma_\pi(p=0, m_i, M_u) \quad (8)$$

stays equal to the tree-level pion mass ($M_\pi \stackrel{!}{=} m_\pi$). The fermionic contribution in the self-energy $\Sigma_\pi(p=0)$ is

$$\Sigma_\pi^F(p=0) = -2g_F^2 T_F(M_u), \quad (9)$$

where $M_u = g_F x/2$, and $T_F(M_u)$ the fermion tadpole defined in Appendix B.

Using the expression of the tree-level pion mass the equation above results in a ‘‘gap’’ equation for the effective mass

$$m^2 = -m_0^2 + \Sigma_\pi(p=0, m_i(m^2), M_u). \quad (10)$$

We introduce the expression above for the effective mass in the expression of the tree-level pion mass. For all the other tree-level propagator masses m_i appearing in the self-energy we replace the effective mass with the pion’s mass using its tree-level expression. Thus we arrive at the following gap-equation for the pion mass

$$m_\pi^2 = -m_0^2 + (4f_1 + 2f_2)x^2 + 4f_1y^2 + 2gy + \Sigma_\pi(p=0, m_i(m_\pi), M_u). \quad (11)$$

This is the first equation from the set of equations used for the parametrization at $T = 0$ and has a distinctive role in our investigation because in the thermodynamical calculation one has to solve its T -dependent counterpart in order to determine $m_\pi(T)$.

The next 2 equations require that the one-loop pole mass of the kaon and eta are equal to the corresponding physical masses. The one-loop equation for the kaon and eta pole masses read (see [7] for their derivation):

$$M_K^2 = -m_0^2 + 2(2f_1 + f_2)(x^2 + y^2) + 2f_2y^2 - \sqrt{2}x(2f_2y - g) + \text{Re} \{ \Sigma_K(p^2 = M_K^2, m_i) \}, \quad (12)$$

$$M_\eta^2 = \frac{1}{2} \text{Re} \left\{ m_{\eta_{xx}}^2 + \Sigma_{\eta_{xx}}(p^2 = M_\eta^2, m_i) + m_{\eta_{yy}}^2 + \Sigma_{\eta_{yy}}(p^2 = M_\eta^2, m_i) \right. \\ \left. - \sqrt{(m_{\eta_{xx}}^2 + \Sigma_{\eta_{xx}}(p^2 = M_\eta^2, m_i) - m_{\eta_{yy}}^2 - \Sigma_{\eta_{yy}}(p^2 = M_\eta^2, m_i))^2 + 4(m_{\eta_{xy}}^2 + \Sigma_{\eta_{xy}}(p^2 = M_\eta^2, m_i))^2} \right\}. \quad (13)$$

The fermionic contribution to the self-energies of the kaon and of the different components in the $x - y$ mixing sector are:

$$\Sigma_K^F(p) = -g_F^2 [T_F(M_u) + T_F(M_s) - (p^2 - (M_u - M_s)^2)I_F(p, M_u, M_s)], \quad (14)$$

$$\Sigma_{\eta_{xx}}^F(p) = -g_F^2 [2T_F(M_u) - p^2 I_F(p, M_u)], \quad \Sigma_{\eta_{yy}}^F(p) = -g_F^2 [2T_F(M_s) - p^2 I_F(p, M_s)], \quad \Sigma_{\eta_{xy}}^F(p) = 0, \quad (15)$$

where the fermionic bubble integral I_F is given in Appendix B. We implemented the FAC principle for the kaon by requiring additionally $\Sigma(p^2 = M_K^2) = 0$. The gap equation for the pion together with these three equations are sufficient to determine m_0^2, f_1, f_2 and g , if we know x, y and g_F . The tree-level PCAC equation fixes $x = f_\pi$. Then the Yukawa coupling is obtained from the tree-level relation $g_F = 2M_u/x$, where M_u is the non-strange constituent quark mass. With the value of g_F fixed we determine y from the strange constituent quark mass $y = \sqrt{2}M_s/g_F$. The values of the external fields are determined from the two equations of state (4) and (5).

We are forced to use the tree-level quark masses because the one-loop quantum correction to it turned out to be very large. This could be kept reasonably small only by using unrealistically low mass values for the tree-level constituent quarks.

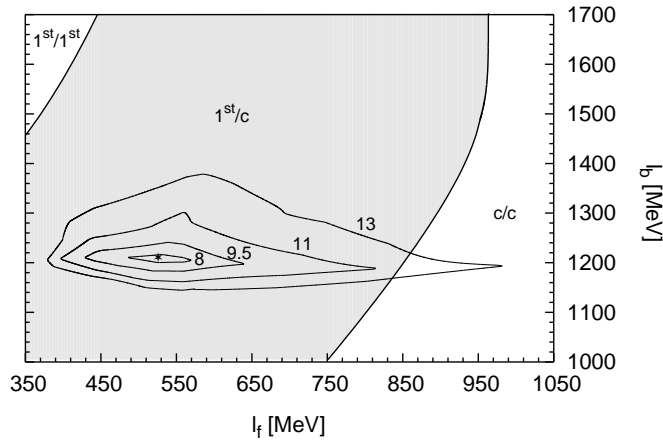


FIG. 1: Contour levels for the quantity R (Eq. (16)) which gives the average percentage for the deviation of the predicted spectrum from the physical one. Shown is also the order of the phase transition on the $T = 0/\mu_B = 0$ axes of the $T - \mu_B$ -plane as a function of the fermionic and bosonic renormalization scale l_f and l_b (c stands for cross-over).

Since we are working with one-loop self-energies, two renormalization scales emerge, one for the renormalization of bosonic integrals, l_b and one for fermionic integrals, l_f . The parameters were determined as functions of these renormalization scales l_b and l_f using as input the values of the physical quantities $m_\pi = 138$ MeV, $m_K = 495.6$ MeV, $m_\eta = 547.8$ MeV, $f_\pi = 93$ MeV, $M_u = 313$ MeV and $M_s = 530$ MeV. The values of the constituent quark masses are related to the masses of the baryon octet components as $M_u \approx M_N/3$ and $M_s \approx (M_\Lambda + M_\Sigma)/2 - 2M_u$. Constraints on the values of l_b and l_f can be obtained by confronting the predicted part of the tree-level and one-loop level mass spectrum with the physical data. To quantify the deviation a quantity is introduced such to reflect the best the spirit of our parametrization

$$R = \frac{1}{|T|} \sum_{i \in T} \frac{|m_i^{\text{tree}} - m_i^{\text{phys}}|}{m_i^{\text{phys}}} + \frac{1}{|L|} \sum_{i \in L} \frac{|m_i^{\text{tree}} - m_i^{\text{1-loop}}|}{m_i^{\text{tree}}}, \quad (16)$$

where $T = \{\eta, \eta', a_0, f_0, \sigma\}$, $L = \{\eta', a_0, \kappa, f_0\}$ and $|T| = 5$, $|L| = 4$. Since the propagator masses that enter the one-loop integrals and determine the quantum corrections are the tree-level masses we measure their average deviation from a given physical spectrum. We also included into the test quantity, R the average deviation of the one-loop masses from the tree-level ones. The one-loop masses are determined from the corresponding propagators through the equation $\text{Re} iG_i^{-1}(p^2 = m_{i,1\text{-loop}}^2) = 0$. There are two notable omissions from the right hand side of Eq. (16). $m_\sigma^{\text{1-loop}}$ is omitted because in a relatively large range of the $l_f - l_b$ -space to be scanned $\text{Re} iG_\sigma^{-1}(p^2 = m_{\sigma,1\text{-loop}}^2) = 0$ has no solution. m_κ^{tree} is omitted because it is actually independent of l_b and l_f . This becomes evident if we use the tree-level relation $m_{\kappa,\text{tree}}^2 = (m_K^2 f_K - m_\pi^2 f_\pi)/(f_K - f_\pi)$ where at tree-level $f_K = x/2 + y/\sqrt{2}$ and according to the parametrization above neither x nor y depend on l_b and l_f ¹. The pseudoscalar physical spectrum used as a reference is completed by $m_{\eta'} = 958$ MeV. As for the scalars, it is still not clear which mesons form the lightest nonet. Possible candidates are the isoscalar σ and $f_0(980)$, the isovector $a_0(980)$ and the isospinor $\kappa(900)$. For the isoscalar masses we choose $m_\sigma = 700$ MeV and $m_{f_0} = 1370$ MeV, because this parametrization of the model cannot accommodate an f_0 lighter than 1 GeV.

The contour plot of the average percentage for the deviation from the physical spectrum measured by R can be seen in Fig. 1. Based on this plot we have chosen the point marked with a star in the figure for which $l_b = 520$ MeV and $l_f = 1210$ MeV. At this point the 1-loop sigma mass can be obtained using the pole-mass definition given above and one obtains $m_\sigma = 614.2$ MeV. The one-loop mass of f_0 is $m_{f_0} = 1210.9$ MeV. Around this optimal point the quantity R can be completed by the contribution of the one-loop mass of the σ meson and the new analysis confirms the choice of l_B and l_f given above.

As indicated in Fig. 1 the order of the phase transition on the axes of the $\mu_B - T$ plane turns out to be sensitive to the value of the renormalization scales. It is very interesting to note, that the requirement of minimal deviation from the physical spectrum results in values of the renormalization scales for which the transition is of first order on the $T = 0$ axis and of cross-over nature on the $\mu_B = 0$ axis of the $\mu_B - T$ phase diagram. This feature turned out to be independent of the way we quantify this deviation, that is the way we define the quantity R . In conclusion, the most reliable parametrization of this model positively predicts the existence of the CEP.

¹ Note, that with this parametrization the kaon decay constant turns out to be $f_K = (1 + M_s/M_u)f_\pi/2 = 125.23$ MeV which is 10% larger than the physical value

III. THE PHASE DIAGRAM IN THE $m_{u,d} - m_s - \mu_B$ SPACE

In order to determine the order of the phase transition in the $m_{u,d} - m_s - \mu_B$ space we have to determine the temperature dependence of the order parameters. This is obtained by solving the two equations of state and the gap equation which form a set of coupled equations:

$$0 = -\epsilon_x + m^2x + 2gxy + 4f_1xy^2 + (4f_1 + 2f_2)x^3 + \sum_i J_i t_i^x T_B^\beta(m_i(m_\pi)) - 4g_F M_u T_F^\beta(M_u) + \Delta m^2 x, \quad (17)$$

$$0 = -\epsilon_y + m^2y + gx^2 + 4f_1x^2y + 4(f_1 + f_2)y^3 + \sum_i J_i t_i^y T_B^\beta(m_i(m_\pi)) - 2\sqrt{2}g_F M_s T_F^\beta(M_s) + \Delta m^2 y, \quad (18)$$

$$m_\pi^2 = -m_0^2 + (4f_1 + 2f_2)x^2 + 4f_1y^2 + 2gy + \Sigma_\pi(p=0, m_i(m_\pi), M_u). \quad (19)$$

J_i stand for the isospin multiplicity factors which are $J_{\pi,a_0} = 3$, $J_{K,\kappa} = 4$, and $J_{\eta,\eta',\sigma,f_0} = 1$. The explicit renormalized expressions of the temperature dependent integrals $T_{B,F}^\beta(m)$ are given in Appendix B. In the notation above we made explicit that the tree-level bosonic masses depend on the pion mass determined by the gap-equation. A first order phase transition is recognized by the multivaluedness in a given temperature and/or chemical potential range of either of the two vacuum expectation values. The point where a first order phase transition goes over into a cross-over is identified as a second order phase transition point.

A. The surface of second order phase transition points

In order to obtain the surface of the second order phase transition points in the $m_{u,d} - m_s - \mu_B$ space we have to determine the variation of the parameters of the Lagrangian with the pion and kaon masses. In addition to the mass of eta and the decay constant of the pion, the constituent quark masses are also used in the parametrization, so their m_π and m_K dependence is required as well. For f_π and m_η we use the formulas of the CHPT in the large N_c limit at $\mathcal{O}(1/f^2)$ as in Ref. [7]

$$f_\pi = f \left(1 + 4L_5 \frac{m_\pi^2}{f^2} \right), \quad (20)$$

$$m_\eta^2 = \frac{4m_K^2 - m_\pi^2}{3} + \frac{32}{3}(2L_8 - L_5) \frac{(m_K^2 - m_\pi^2)^2}{f^2}. \quad (21)$$

The values of the constants are: $L_5 = 2.0152 \cdot 10^{-3}$, $L_8 = 8.472 \cdot 10^{-4}$ and $f = 91.32$ MeV. These quantities are independent of m_π and m_K , and were determined in Ref. [7] from the condition that at the physical point the pion and kaon decay constants and m_η take their physical values.

In a simple constituent quark picture the constituent quark masses are related to the values of the baryon masses whose dependence on m_π and m_K is obtained using the formulas of the CHPT for baryons at $\mathcal{O}(q^3)$ [16] (q denotes the momentum). To this order in the chiral expansion the masses of the baryon octet are given by

$$M_B = M_0 - 2b_0(m_{\pi,2}^2 + m_{K,2}^2) + b_D \gamma_B^D + b_F \gamma_B^F - \frac{1}{24\pi f^2} [\alpha_B^\pi m_\pi^3 + \alpha_B^K m_K^3 + \alpha_B^\eta m_\eta^3], \quad (22)$$

where $B \in \{N, \Sigma, \Lambda, \Xi, \}$. $\alpha_B^\pi, \alpha_B^K, \alpha_B^\eta$ are simple expressions of two low energy constants D and F , the coefficients characterizing the lowest order baryon Lagrangian (see Eq. (6.9a) of Ref. [16] for the explicit expressions). The expressions of γ_B^D and γ_B^F read as:

$$\gamma_N^D = \gamma_\Xi^D = -4m_{K,2}^2, \quad \gamma_N^F = -\gamma_\Xi^F = 4(m_{K,2}^2 - m_{\pi,2}^2), \quad \gamma_\Sigma^D = -4m_{\pi,2}^2, \quad \gamma_\Lambda^D = -4m_{\eta,2}^2, \quad \gamma_\Sigma^F = \gamma_\Lambda^F = 0. \quad (23)$$

The subscript 2 refers to the fact that the squared meson mass is taken at the lowest, $\mathcal{O}(q^2)$ order. Originally these lowest-order mass expressions appear also in the $\mathcal{O}(f^{-2})$ term, but it is allowed to replace them with their physical values. For the $\mathcal{O}(f^0)$ piece we use $m_{M,2}^2 = m_M^2 - 8m_\pi^4 f^{-2}(2L_8 - L_5)$ for $M = \pi, K$ and Eq. (21) to relate the lowest-order mass with the physical one. Note, that due to the lowest order Gell-Mann–Okubo relation the first term in Eq. (21) is $m_{\eta,2}^2$.

The unknown constants are M_0 , the baryon mass in the chiral limit and b_0, b_D, b_F the coefficients of the lowest order symmetry breaking part (contact contribution). Since M_0 and b_0 appear in the same combination for all the masses an additional relation is needed in order to disentangle them. This relation is usually chosen to be the so-called nucleon sigma-term defined in terms of the proton matrix element of the 11 component of the sigma commutator

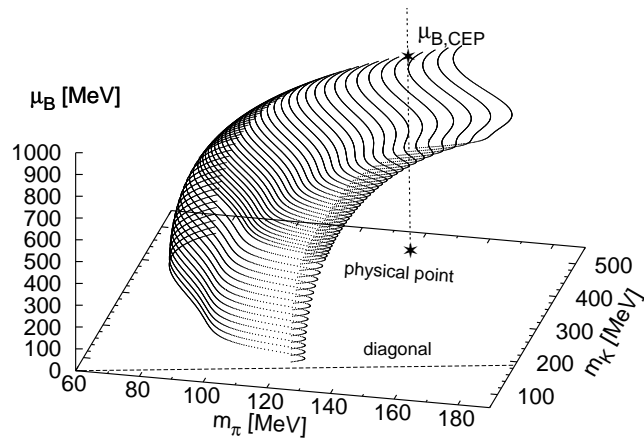


FIG. 2: The surface of second order phase transition points.

$\sigma_{\pi N} = \langle p | \sigma_{11}(0) | p \rangle / 2M_p$, where M_p is the proton mass.² At $\mathcal{O}(q^3)$ the sigma-term reads [16]

$$\sigma_{\pi N} = -2(2b_0 + b_D + b_F)m_{\pi,2}^2 - \frac{m_{\pi}^2}{64\pi f^2} \left[4\alpha_N^{\pi} m_{\pi} + 2\alpha_N^K m_K + \frac{4}{3}\alpha_N^{\eta} m_{\eta} \right]. \quad (24)$$

The four constants are determined from the expressions of M_N , M_{Ξ} , $(M_{\Sigma} + M_{\Lambda})/2$ and $\sigma_{\pi N}$ using as input $D = 0.8$, $F = 0.5$, $M_N = 938.92$ MeV, $M_{\Sigma} = 1193.15$ MeV, $M_{\Lambda} = 1115.683$ MeV, $M_{\Xi} = 1317.915$ MeV and $\sigma_{\pi N} = 45$ MeV. The obtained values are: $M_0 = 939.82$ MeV, $b_0 = -0.869$ GeV⁻¹, $b_D = 0.0363$ GeV⁻¹ and $b_F = -0.582$ GeV⁻¹. We keep these values fixed when determining the constituent quark masses on the $m_{\pi} - m_K$ mass plane as $M_u = M_N/3$ and $M_s = (M_{\Lambda} + M_{\Sigma})/2 - 2M_u$. Then at fixed values of the renormalization scales the parametrization described in sec. II is performed for each point of the mass plane.

The result obtained after finding the nature of the phase transition by solving Eqs. (17),(18),(19) is displayed in Fig. 2. The second order surface is shown only in a restricted region of the mass plane for two reasons. On the one hand the parametrization breaks down close to the diagonal of the mass-plane. Along the diagonal the masses become degenerate and we cannot determine the same number of parameters from fewer equations. On the other hand, for large values of the kaon masses $m_K > 400$ MeV we see that the surface bends away from the $m_{\pi} = 0$ axis (apparently no crossing occurs). This is an unphysical behavior since within the linear sigma model, that is without fermions, it was shown in Ref. [7] that for $\mu_B = 0$ the boundary of the first order transition region approaches the $m_{\pi} = 0$ axis, allowing to locate there a tricritical point (TCP). This anomalous behavior originates from the way the baryon masses depend on m_K : all of them start to decrease with increasing m_K , for m_N at around $m_K = 300$ MeV, for m_{Λ} at $m_K \approx 400$ MeV and for m_{Σ} and m_{Ξ} this occurs at around $m_K = 500$ MeV. This means that above $m_K = 400$ MeV one can not trust the $\mathcal{O}(q^3)$ formulas of the CHPT for the baryon masses. Based on the m_K dependence of the baryon masses presented in [17] we can say that had we used the more complicated $\mathcal{O}(q^4)$ formulas we would have observed the bending away of the surface from the $m_{\pi} = 0$ axis at around $m_K = 600$ MeV. The result of Ref. [7] shows that even at this value of the kaon mass we would be far from the scaling region of the TCP.

We can see that the surface grows out perpendicularly from the mass plain ($\mu_B = 0$). This means that the critical points $\mu_B^c(m_{\pi}, m_K)$ which are close to the mass plane are extremely sensitive to the values of m_{π} and m_K . This was observed in lattice simulation using imaginary chemical potential, where this is the region which is traversed when performing the analytical continuation to real chemical potential [11]. We can also see that the tangent plane to the surface has a decreasing angle with the mass plane as one approaches the critical point which corresponds to the physical masses. Here the dependence of $\mu_B^c(m_{\pi}, m_K)$ on the masses is milder.

B. The CEP at the physical point of the mass-plane

Now we turn back to the physical point in order to study the location of the CEP in the $\mu_B - T$ -plane. There are many effective model studies published in the literature (see Ref. [18] for an extensive list), the major part of them was done with two flavors.

² The sigma commutator is defined as $\sigma^{ab}(x) = [Q_A^a(x_0), [Q_A^b(x_0), \mathcal{H}_{sb}(x)]]$, where $Q_A^a(x_0)$ is the axial charge operator and $\mathcal{H}_{sb} = \bar{q}\mathcal{M}q$ is the chiral symmetry breaking term of the QCD Hamiltonian ($\mathcal{M} = \text{diag}(m_u, m_d, m_s)$).

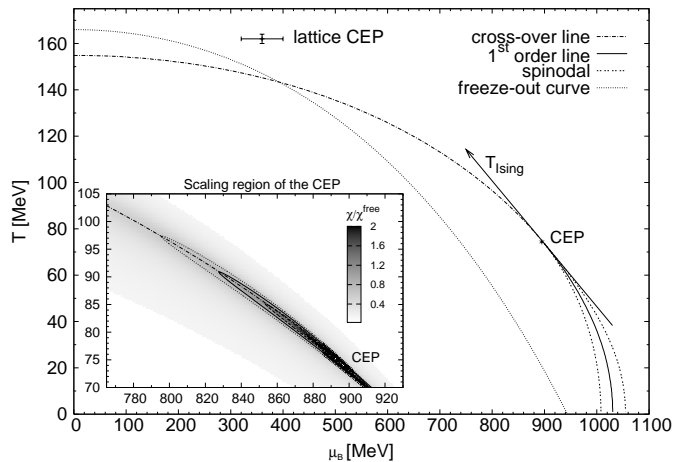


FIG. 3: The phase diagram corresponding to the point denoted with a star in Fig. 1. Shown are the universal chemical freeze-out line from Ref. [24] and the CEP obtained in the lattice [9]. The arrow at the CEP shows the temperature direction of the 3d Ising model.

As we have discussed in Sec. II, reasonable values, namely $l_f = 520$ MeV and $l_b = 1210$ MeV have been chosen for the renormalization scales. In the cross-over region we determined for increasing values of μ_B the pseudo-critical temperature T_c through the location of the peak of the derivative of the non-strange order parameter x with respect to T . The peak diverges at the CEP. For higher values of μ_B in the first order transition region the spinodals were defined as the two turning points of the two-valued order parameter x as function of μ_B at fixed T . Since we have not calculated the effective potential, we defined the first order line through the points between the two spinodals, where $x(\mu_B)$ has an inflection point at fixed T . This line together with the two spinodals, plus the cross-over transition line and the location of the CEP ($T_{\text{CEP}} = 74.83$ MeV, $\mu_{B,\text{CEP}} = 895.38$ MeV) can be seen in Fig. 3. The fact that the CEP value of the temperature is smaller and that of the μ_B is larger than what is found on the lattice ($T_{\text{CEP}} = 162 \pm 2$ MeV and $\mu_{B,\text{CEP}} = 360 \pm 40$ MeV, cf. [9]) seems to be a common feature of all results obtained in the linear sigma model and the Nambu–Jona-Lasinio model.

In Fig. 3 we display also the universal chemical freeze-out curve of Ref. [24] which is parametrized as $T(\mu_B) = a - b\mu_B^2 - c\mu_B^4$, where $a = 0.166$ GeV, $b = 0.139$ GeV $^{-1}$ and $c = 0.053$ GeV $^{-3}$. We can see that for $\mu_B > 400$ MeV our phase transition line lies above the curve which separates a region dominated by inelastic processes (high-T region) from a region dominated by elastic processes. The parameters of the freeze-out curve (μ_B and T) reproduce in thermal models the particle yields measured in experiments performed at different beam energies. It is called universal because is obtained from the condition that the average energy per average number of hadrons is approximately 1 GeV. The sensitivity of this curve to other freeze-out conditions is studied in Ref. [24]. It is expected that the chemical freeze-out takes place below the true phase transition line. In the resonant gas model with rescaled mass spectrum such as to reproduce $m_\pi = 770$ MeV of the lattice simulation with 2 flavor QCD using Taylor expansion of the fermion determinant, the line of fixed energy density reproduces the transition line of the lattice. The set of physical resonances expected to appear in the (2+1)-flavor QCD results in a line of fixed energy density which is close to the chemical freeze-out line in the meson dominated region ($\mu_B < 400$ MeV) and lies above it in the baryon dominated region ($\mu_B > 400$ MeV) [25].

There are some quantities like the width of the peak of the chiral susceptibility and the curvature of the cross-over line at $\mu_B = 0$, which can be compared with their values measured on the lattice. The width of the chiral susceptibility as a function of T gives information on the strength of the cross-over transition. The continuum result of Ref. [1] is $\Delta T_c(\chi_{\bar{\psi}\psi}) = 28(5)(1)$ MeV. We obtain $\Delta T_c(x\chi) = 15.5$ MeV which means that the transition is more abrupt in our case³. It is interesting to remark that for the simulation of Ref. [9] in which the CEP was found the width is about an order of magnitude smaller than in the continuum limit [19]. Then a natural expectation is that in the continuum limit the location of the CEP would move to higher values of μ_B , that is a larger value of μ_B would be required to turn the phase transition into a first order type if one starts with a weak cross-over at $\mu_B = 0$.

Another quantity which can be compared is the curvature at $\mu_B = 0$ which is measured by $C := T_c \frac{d^2 T_c}{d\mu_B^2} \Big|_{\mu_B=0}$. Our value $C = -0.09$ is 35 – 40% larger than the lattice result $C = -0.058(2)$ for $N_f = 2 + 1$ of Ref. [9]. Our pseudo-

³ It is worth to note, that the susceptibility which can be defined in this model, namely $\chi = dx/d\epsilon_x$ can be connected with the chiral susceptibility of the light quarks $\chi_{\bar{\psi}\psi} = d\langle\bar{\psi}\psi\rangle/dm_u$. This is based on the following relations: $\langle\bar{\psi}\psi\rangle \sim x$, $m_\pi^2 = B_0 m_u$ (lowest order relation in CHPT) and $m_\pi^2 = \epsilon_x/x$ (Goldstone theorem). From these immediately follows: $\chi_{\bar{\psi}\psi} \sim x\chi$.

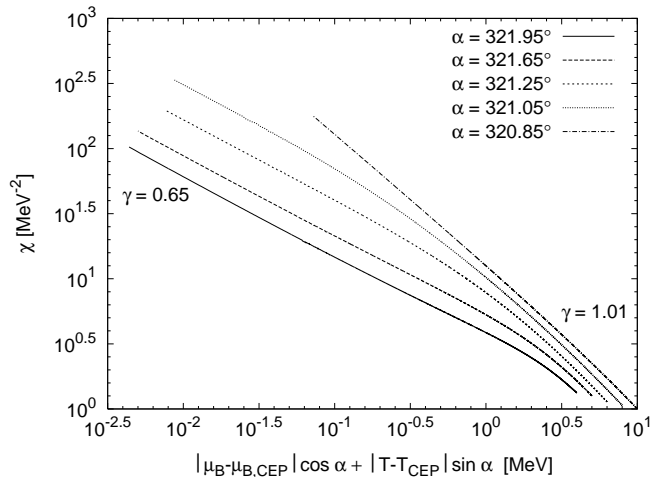


FIG. 4: The chiral susceptibility as a function of the distance from the CEP. For the sake of visibility, the lines from left to right were shifted to the left by 0, $10^{0.1}$, $10^{0.2}$, $10^{0.3}$ and $10^{0.4}$, respectively.

critical temperature at vanishing chemical potential $T_c = 154.84$ MeV is quite close to $T_c = 164(2)$ MeV obtained in Ref. [9] but is even closer to what was obtained in the continuum limit in Ref. [1], namely $T_c = 151(3)$ MeV. A collection of curvatures obtained in different lattice approaches and for different flavor numbers is given in Ref. [20], where it was observed that the curvature is considerably decreased if the coefficient g of the determinant term in the Lagrangian decreases with the temperature. The rapid decrease of the anomaly near the chiral transition temperature is indicated by lattice simulations. In NJL model the T -dependence of g can be extracted by fitting the lattice result on the topological susceptibility with an analytic formula of the susceptibility [21]. Following Ref. [22] we considered $g(T) = \exp(-(T/T_0)^2)$. As a consequence the curvature was reduced to $C = -0.08$. This means that the restoration of the $U_A(1)$ symmetry has an influence on the shape of the crossover transition line and on the location of the CEP. More detailed dependence of g on T and μ_B is needed in order to assess this influence on the location of the CEP.

We have studied the shape of the critical region based on the chiral susceptibility $\chi = dx/d\epsilon_x$. This is important in phenomenology, since according to Ref. [26] if the critical region is larger than the region where the so-called focusing effect (see Ref. [27]) is realized, then the interactions cannot be neglected and the use of resonance gas model could be questionable. We found that the critical region is heavily stretched in the direction of crossover transitions line as shown in the smaller picture on Fig.3, in which we depicted the ratio χ/χ^{free} , where χ^{free} is the chiral susceptibility of a free massless quark gas, given by $\chi^{\text{free}} = T^2/6 + \mu_B^2/(18\pi^2)$. The contours shown are 1.2, 0.8, 0.6 from inside out. The highest values are concentrated around the pseudo-critical line in a 1 – 2 MeV wide elongated region. The shape of the critical region is similar to what was observed based on quark number susceptibility in Ref. [23] in the two-flavor effective QCD.

We determined the mapping of the temperature axis of the Ising model onto the $\mu_B - T$ plane at the CEP which is in the universality class of a 3d Ising model. To do this, we have measured, through the relation $\chi \sim (|\mu_B - \mu_{B,\text{CEP}}| \cos \alpha + |T - T_{\text{CEP}}| \sin \alpha)^{-\gamma}$, the critical exponent of the chiral susceptibility along different directions pointing toward the CEP and characterized by an angle $\alpha \in [0, 360^\circ]$ measured from the positive μ_B axis. Going with increasing μ_B along the direction tangent to the cross-over line at the CEP having $\alpha = 320.85^\circ$ we obtained $\gamma = 1.01$, which corresponds to the mean-field exponent 1. This direction corresponds to the temperature axis of the Ising model and it is shown in Fig. 3 by the arrow at CEP. From directions not parallel to the tangent line $\gamma \sim 0.64$, as was found in Ref. [23].

Below we present in details how the direction corresponding to the Ising temperature axis was found. According to the Landau-Ginzburg type analysis of Ref. [23], the critical region of the CEP is splitted into two scaling regions. One of them contains path which are asymptotically parallel to the tangent line of the cross-over curve at the CEP along which $\gamma = 1$ (mean field exponent), while the other one is the complement region of the first where $\gamma = 2/3$. In accordance with these, we found that by choosing a path which is near the asymptotically parallel direction, the chiral susceptibility as function of the distance from the CEP consists of two straight lines in a log-scale plot having slopes 1 and 2/3, respectively. Moreover, as we approach the direction of the tangent line to the critical curve at the CEP, the range of the line with slope 2/3 shrinks and the range of the line with slope 1 grows, as one can see in Fig. 4. Asymptotically parallel to the tangent line there is no more crossing of scaling regions, the path remains in the region characterized by $\gamma = 1$.

IV. CONCLUSION

A resummed perturbation theory was used for the parametrization of the $SU(3)_L \times SU(3)_R$ chiral quark model with one-loop accuracy using as input the physical pseudoscalar sector and the masses of the constituent quarks. We

found that in a large range of the bosonic and fermionic renormalization scales, within the parametrization scheme used the model gives 1st order transition on the $T = 0$ axis and crossover type transition on the $\mu_B = 0$ axis of the $\mu_B - T$ -plane at the physical point of the $m_\pi - m_K$ mass-plane. The renormalization scales were fixed by the requirement of minimal deviation of the predicted mass spectrum from the physical one and the critical end point was located at $\mu_{B,CEP} = 895.38$ MeV and $T_{CEP} = 74.83$ MeV. The location and the shape of the critical region of the CEP were confronted with other results from the literature. We consider that in an effective model a finite answer for the actual location of the CEP can be given only by supplementing the chiral nature of the transition with other aspects of a true deconfinement transition, like the influence of the confinement, which can be taken into account through the Polyakov loop potential and the dependence of the axial anomaly on the temperature and density. For this more detailed knowledge of these phenomena is needed.

We also studied the surface of the second order phase transition points in the $m_\pi - m_K - \mu_B$ space using chiral perturbation theory for meson and baryons in order to continue the model's parameters from their value at the physical point. This surface rises from the boundary of the first order phase transition region on the $m_\pi - m_K$ plane as the baryonic chemical potential is increased. We found that the surface has positive curvature bending monotonically towards the physical point of the mass-plane.

Acknowledgment

Work supported by the Hungarian Scientific Research Fund (OTKA) under contract number T046129. Zs. Sz. is supported by OTKA Postdoctoral Grant no. PD 050015. This work profited from useful discussions with Z. Fodor and T. Herpay and also from suggestions by S. Katz and A. Patkós. We thank S. Katz for performing a simulation which estimates the width of the chiral susceptibility for the single volume $12^3 \times 4$ and lattice action used in [9].

APPENDIX A: CALCULATION IN THE MIXING SECTOR

Not all of the scalar and pseudoscalar fields of the Lagrangian are mass eigenstates, there is a mixing between the singlet and the octet states. Since physically only mass eigenstates can propagate we have to diagonalize the propagators encountered when calculating the self-energies. In the mixing, $x - y$ sector, the diagonal matrix \tilde{G} containing the tree-level physical propagators are obtained through an orthogonal transformation performed with the matrix $O = \begin{pmatrix} \cos \theta & \sin \theta \\ -\sin \theta & \cos \theta \end{pmatrix}$ ($\tan 2\theta = 2m_{xy}^2/(m_{xx}^2 - m_{yy}^2)$) as $\tilde{G} = OGO^T$. Following the convention of Ref. [14] (see Eqs. (18) and (20)) we define $\tilde{G}_S = \text{diag}(G_\sigma, G_{f_0})$ ($\tilde{G}_P = \text{diag}(G_{\eta'}, G_\eta)$) in the (pseudo)scalar sector. It is easy to show, that one has $\sin 2\theta_P = 2m_{\eta xy}/\sqrt{(m_{\eta xx}^2 - m_{\eta yy}^2)^2 + 4m_{\eta xy}^4}$, $\cos^2 \theta_P = [1 + (m_{\eta xx}^2 - m_{\eta yy}^2)/\sqrt{(m_{\eta xx}^2 - m_{\eta yy}^2)^2 + 4m_{\eta xy}^4}]/2$ in the pseudoscalar sector and $\sin 2\theta_S = -2m_{\sigma xy}/\sqrt{(m_{\sigma xx}^2 - m_{\sigma yy}^2)^2 + 4m_{\sigma xy}^4}$, $\cos^2 \theta_S = [1 - (m_{\sigma xx}^2 - m_{\sigma yy}^2)/\sqrt{(m_{\sigma xx}^2 - m_{\sigma yy}^2)^2 + 4m_{\sigma xy}^4}]/2$ in the scalar sector. These expressions are to be used when expressing the xx , xy and yy components of the internal propagators of Feynman diagrams. In the pseudoscalar sector one has

$$G_{xx}^P = G_{\eta'} \cos^2 \theta_P + G_\eta \sin^2 \theta_P, \quad G_{yy}^P = G_{\eta'} \sin^2 \theta_P + G_\eta \cos^2 \theta_P, \quad G_{xy}^P = (G_{\eta'} - G_\eta) \sin \theta_P \cos \theta_P, \quad (\text{A1})$$

and similarly for the scalar sector with the replacements $G_{\eta'} \rightarrow G_\sigma$, $G_\eta \rightarrow G_{f_0}$ and $\theta_P \rightarrow \theta_S$. By doing this in the non-mixing sector we obtain the self-energies in terms of the physical propagators, while in the mixing sectors we obtain the xx , xy and yy components of the self-energies. In this latter sector an additional diagonalization is required to obtain the self-energies for the mass eigenstates η' , η , f_0 and σ .

APPENDIX B: INTEGRALS

The one-loop fermionic integrals encountered in the calculation are the tadpole $T_F^\beta(m_q)$ and the bubble $I_F(p, m_q)$. In the imaginary-time formalism the tadpole integral for a quark with mass m_q is defined as:

$$\langle \bar{q}q \rangle = -4m_q iT \sum_{n=-\infty}^{\infty} \int \frac{d^3k}{(2\pi)^3} \frac{i}{\omega_n^2 - \vec{k}^2 - m_q^2} =: -4m_q T_F^\beta(m_q), \quad (\text{B1})$$

where $\omega_n = (2n + 1)\pi T$. After renormalization at finite temperature one has

$$T_F^\beta(m_q) = \frac{m_q^2}{16\pi^2} \ln \frac{m_q^2}{l_f^2} + \frac{1}{2\pi^2} \int_{m_q}^{\infty} d\omega \sqrt{\omega^2 - m_q^2} f_F(\omega), \quad (\text{B2})$$

where in terms of the Fermi-Dirac distributions for quarks and antiquarks $f_F^\pm(\omega) = 1/(\exp(\beta(\omega \mp \mu_q)) + 1)$, $f_F(\omega)$ is given by $f_F(\omega) = -\frac{1}{2} [f_F^+(\omega) + f_F^-(\omega)]$ and $\mu_q = \mu_B/3$. (The bosonic tadpole $T_B^\beta(m)$ looks exactly the same but with $f_F(\omega)$ replaced by the Bose-Einstein distribution $f_B(\omega) = 1/(\exp(\beta\omega) - 1)$).

There are two types of bubble integrals, the first occurs in the pseudoscalar self-energies and is used in the process of the parametrization while the other gives contribution to the scalar self-energies when calculating the one-loop mass of the scalars. Both are needed only at zero temperature. Their expressions stand here:

$$\begin{aligned} \Sigma_{P/S}(p, m_1, m_2) &= \frac{g_F^2}{2} \text{Tr} \int \frac{d^4 k}{(2\pi)^4} \frac{i\Gamma_{P/S}(\not{k} + m_1)\Gamma_{P/S}(\not{p} - \not{k} + m_2)}{(k^2 - m_1^2)((k-p)^2 - m_2^2)} \\ &= g_F^2 [(p^2 - (m_1 \mp m_2)^2)I(p, m_1, m_2) - T_F(m_1) - T_F(m_2)], \end{aligned} \quad (\text{B3})$$

where for pseudoscalars $\Gamma_P = \gamma_5$ and for scalars $\Gamma_S = -i$. $I(p, m_1, m_2)$ is the expression encountered when calculating a bosonic bubble integral:

$$\begin{aligned} I(p, m_1, m_2) &= \frac{1}{16\pi^2} \left[\ln \frac{m_2^2}{e l_f^2} + \frac{1}{2} \left(1 + \frac{m_1^2 - m_2^2}{p^2} \ln \frac{m_1^2}{m_2^2} \right) \right] \\ &+ \frac{G}{16p^2\pi^2} \begin{cases} -\frac{1}{2} \ln \left| \frac{m_1^2 + m_2^2 - p^2 + G}{m_1^2 + m_2^2 - p^2 - G} \right| - i\pi\Theta(p^2 - (m_1 + m_2)^2), & \text{for } p^2 > (m_1 + m_2)^2, p^2 < (m_1 - m_2)^2, \\ \arctan \frac{p^2 - m_1^2 + m_2^2}{G} + \arctan \frac{p^2 + m_1^2 - m_2^2}{G}, & \text{for } (m_1 - m_2)^2 < p^2 < (m_1 + m_2)^2, \end{cases} \end{aligned} \quad (\text{B4})$$

where $G = |(p^2 - (m_1 + m_2)^2)(p^2 - (m_1 - m_2)^2)|^{1/2}$. For two equal masses the corresponding expression can be easily obtained.

-
- [1] Y. Aoki, Z. Fodor, S. D. Katz, K. K. Szabó, [hep-lat/0609068].
 - [2] Y. Aoki, G. Endrődi, Z. Fodor, S. D. Katz, K. K. Szabó, *Nature* **443**, 675 (2006)
 - [3] F. Karsch, C. R. Allton, S. Ejiri, S. J. Hands, O. Kaczmarek, E. Laermann and C. Schmidt, *Nucl. Phys. Proc. Suppl.* **129-130**, 614 (2004) [hep-lat/0309116].
 - [4] F. Karsch *et al.*, *Nucl. Phys. B (Proc. Suppl.)* **129&130**, 614 (2004) [hep-lat/0309116], see also C. Schmidt, PhD Thesis, Bielefeld University, 2003, available online at <ftp://ftp.uni-bielefeld.de/pub/papers/physik/theory/e6/dissertationen/schmidt.ps.gz>
 - [5] J. T. Lenaghan, *Phys. Rev. D* **63**, 037901 (2001) [hep-ph/0005330].
 - [6] T. Herpay, A. Patkós, Zs. Szép, P. Szépfalusy, *Phys. Rev. D* **71**, 125017 (2005) [hep-ph/0504167].
 - [7] T. Herpay, Zs. Szép, *Phys. Rev. D* **74**, 025008 (2006) [hep-ph/0604086].
 - [8] Z. Fodor, S. D. Katz, *JHEP* 0203 (2002) 014 [hep-lat/0106002].
 - [9] Z. Fodor, S. D. Katz, *JHEP* 0404 (2004) 050 [hep-lat/0402006].
 - [10] S. Ejiri *et al.*, *Prog. Theor. Phys. Suppl.* **153**, 118 (2004) [hep-lat/0312006]
 - [11] O. Philipsen, Ph. de Forcrand, [hep-lat/0607017].
 - [12] M. Lévy, *Nuovo Cim.* **52A**, 23 (1967)
 - [13] L.-H. Chan and R. W. Haymaker, *Phys. Rev. D* **7**, 402 (1973) [nucl-th/9901049].
 - [14] J.T. Lenaghan, D. H. Rischke and J. Schaffner-Bielich, *Phys. Rev. D* **62**, 085008 (2000) [nucl-th/0004006].
 - [15] S. Chiku and T. Hatsuda, *Phys. Rev. D* **58**, 076001 (1998) [hep-ph/9803226].
 - [16] V. Bernard, N. Kaiser, Ulf-G. Meißner, *Int. J. Mod. Phys.* **E4**, 193 (1995) [hep-ph/9501384]
 - [17] M. Frink, U. G. Meißner, I. Scheller, *Eur. Phys. J.* **A24**, 395 (2005) [hep-lat/0501024]
 - [18] M. Stephanov, *Progress of Theoretical Physics Supplement* **153**, 139 (2004) [hep-ph/0402115]
 - [19] S. Katz, private communication.
 - [20] A. Barducci, R. Casalbuoni, G. Pettini, L. Ravagli, *Phys. Rev. D* **72**, 056002 (2005) [hep-ph/0508117]
 - [21] K. Ohnishi, K. Fukushima, K. Ohta, *Phys. Rev. C* **63**, 045203 (2001) [nucl-th/0101062].
 - [22] T. Kunihiro, *Phys. Lett.* **B219**, 363 (1989)
 - [23] Y. Hatta, T. Ikeda, *Phys. Rev. D* **67**, 014028 (2003) [hep-ph/0210284]
 - [24] J. Cleymans, H. Oeschler, K. Redlich, S. Wheaton, *Phys. Rev. C* **73**, 034905 (2006) [hep-ph/0511094]
 - [25] K. Redlich, *Acta Phys. Hung.* **A22**, 343 (2005) [hep-ph/0406250]
 - [26] C. Nonaka and M. Asakawa, *Phys. Rev. C* **71**, 044904 (2005) [nucl-th/0410078]
 - [27] M. Stephanov, K. Rajagopal, E. Shuryak, *Phys. Rev. Lett.* **81**, 4816 (1998) [hep-ph/9806219]